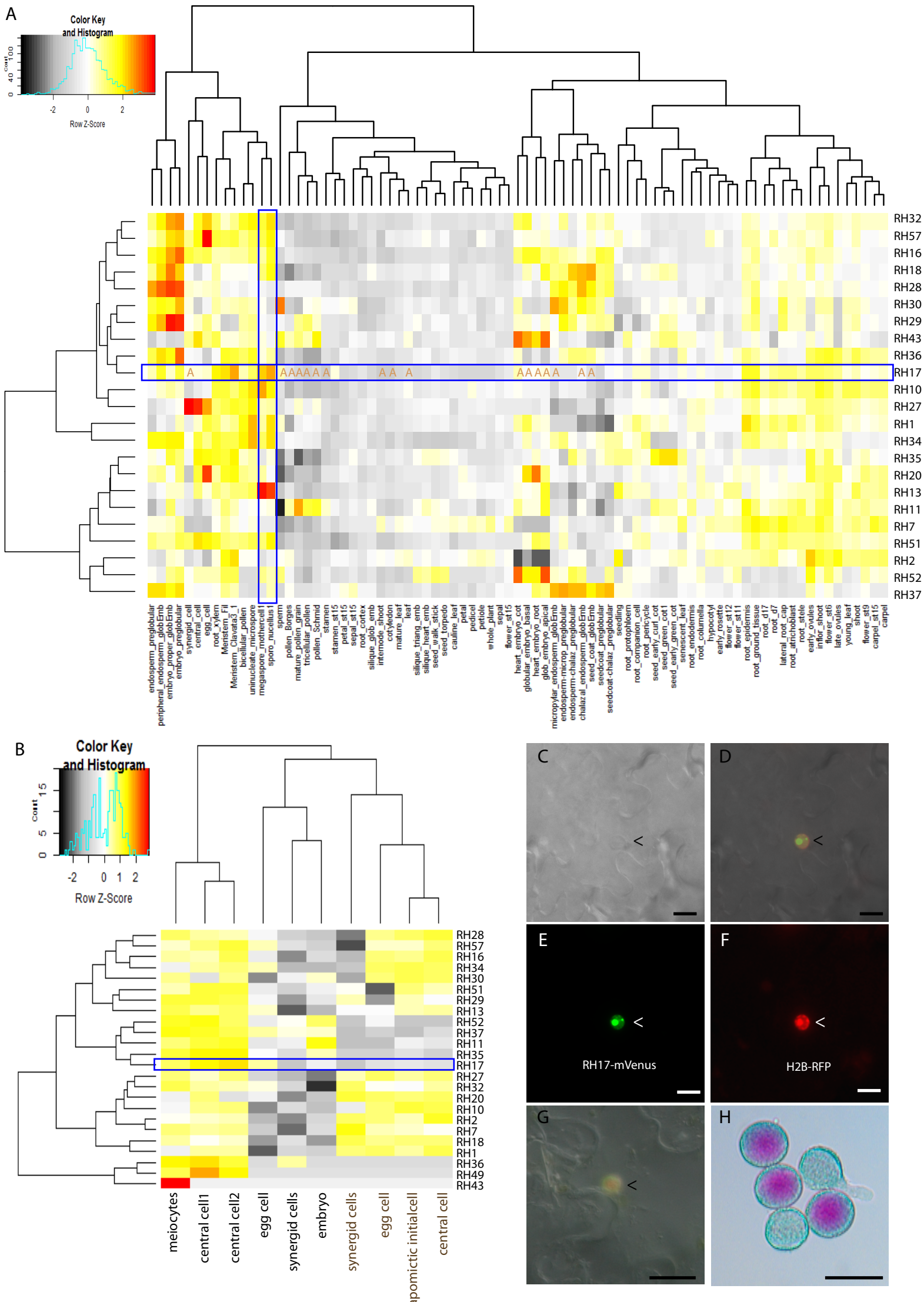
A
Color Key and Histogram
Count
Row Z-Score
RH32
RH57
RH16
RH18
RH28
RH30
RH29
RH43
RH36
RH17
RH10
RH27
RH1
RH34
RH35
RH20
RH13
RH11
RH7
RH51
RH2
RH52
RH37
endosperm_preglobular
peripheral_endosperm_globEmb
embryo_proper_globEmb
embryo_preglobular
synergid_cell
central_cell
egg_cell
root_xylem
Meristem_Fil
Meristem_Clavata3_1
bicellular_pollen
uninucleate_microspore
megaspore_mothercell1
sporo_nucellus1
sperm
pollen_Borges
mature_pollen_grain
tricellular_pollen
pollen_Schmid
stamen
stamen_st15
petal_st15
sepal_st15
root_cortex
silique_glob_emb
internode_shoot
cotyledon
mature_leaf
leaf
silique_triang_emb
silique_heart_emb
seed_walk_stick
seed_torpedo
cauline_leaf
petal
pedicel
petiole
whole_plant
sepal
flower_st15
heart_embryo_cot
globular_embryo_basal
heart_embryo_root
glob_embryo_apical
micropylar_endosperm_globEmb
endosperm-microp_preglobular
endosperm-chalaz_preglobular
chalaz.al_endosperm_globEmb
seed_coat_globEmb
seedcoat_preglobular
seedcoat-chalaz_preglobular
seedling
root_protophloem
root_companion_cell
root_pericycle
seed_early_curl_cot
seed_green_cot1
seed_early_green_cot
senescent_leaf
root_endodermis
root_columella
hypocotyl
early_rosette
flower_st12
flower_st11
root_epidermis
root_ground_tissue
root_d17
root_d7
lateral_root_cap
root_atrichoblast
root_stele
early_ovules
inflor_shoot
flower_st6
late_ovules
young_leaf
shoot
flower_st9
carpel_st15
carpel
B
Color Key and Histogram
Count
Row Z-Score
RH28
RH57
RH16
RH34
RH30
RH51
RH29
RH13
RH52
RH37
RH11
RH35
RH17
RH27
RH32
RH20
RH10
RH2
RH7
RH18
RH1
RH36
RH49
RH43
meiocytes
central cell1
central cell2
egg cell
synergid cells
embryo
synergid cells
egg cell
apomictic initialcell
central cell
C
D
E
RH17-mVenus
F
H2B-RFP
G
H

Fig. S1. Heatmap of expression, subcellular localization, and pollen viability. (A,B) Analysis of expression of DEAD-box RNA helicases with homologies to yeast and human ribosomal binding factors (Liu and Imai, 2018). (A) Heatmap of log2-transformed mean expression values in a total of 74 cell types and tissues in Arabidopsis as used in (Kotliński et al., 2017). (B) Heatmap of normalized log2-transformed read counts from reproductive cell and tissue types of Arabidopsis or *Boechera gunnisoniana* as reported in (Schmidt et al., 2014). (A,B) Hierarchical clustering of genes and samples was based on euclidean distance and agglomerative hierarchical clustering. Red denotes high expression and black low expression. Blue boxes indicate the row of *RH17* expression values and the columns of the megaspore mother cell and surrounding sporophytic nucellus tissues. “A” indicates the absence in the majority of biological replicates evaluated as previously described (Schmidt et al., 2011). (C-G) Subcellular localization of RH17 fused to mVenus by epifluorescence microscopy after transient expression in *Nicotiana benthamiana* leaves under the control of the Arabidopsis *UBIQUTIN10* (*UBI10*) promoter. As control for expression in the nucleus, co-transformation with a construct driving the expression of H2B-RFP under the control of the *UBI10* promoter was applied (Lucas et al., 2013). (C) Cells visualized by differential inference contrast (DIC) microscopy, (E) RH17-mVenus and (F) H2B-RFP localization in the nucleus (arrows), and (D) overlay of DIC, YFP and RFP channels. (G) Colocalization of RH17-mVenus and H2B-RFP in the nucleus (arrow). (H) Analysis of pollen viability analyzed by Alexander Staining (Ross et al., 2010) and light microscopy. Pink staining indicates viable pollen and blue staining aborted pollen. Scale bars are 20 µm.

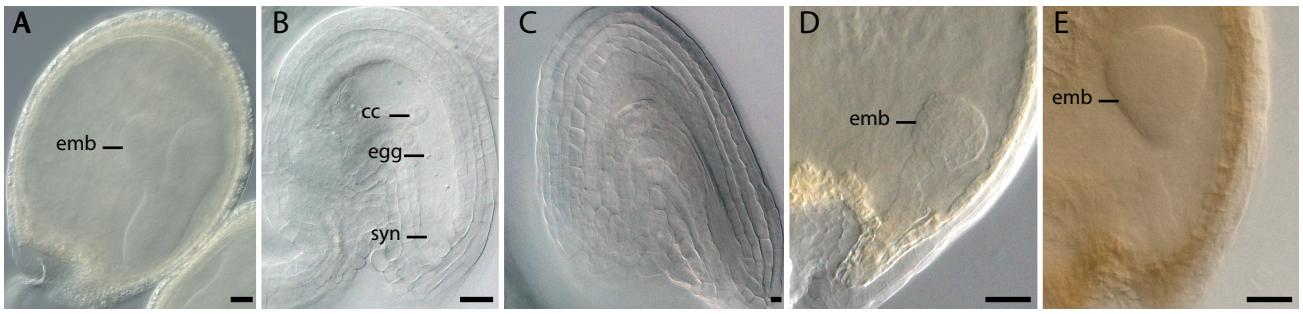

Fig. S2. Morphological investigation of ovule and seed development. (A) Seed with embryo (emb) at torpedo stage of development in the wild-type. Unfertilized or unfertile mature gametophyte (B) and over-proliferated embryo (E) in silique of *rh17-1/RH17* (egg, egg cell; cc, central cell; syn, synergids). Seed with only seed coat formed (C) and over-proliferated embryo (D) in *rh17-2/RH17*. Scale bars are 20 μm.

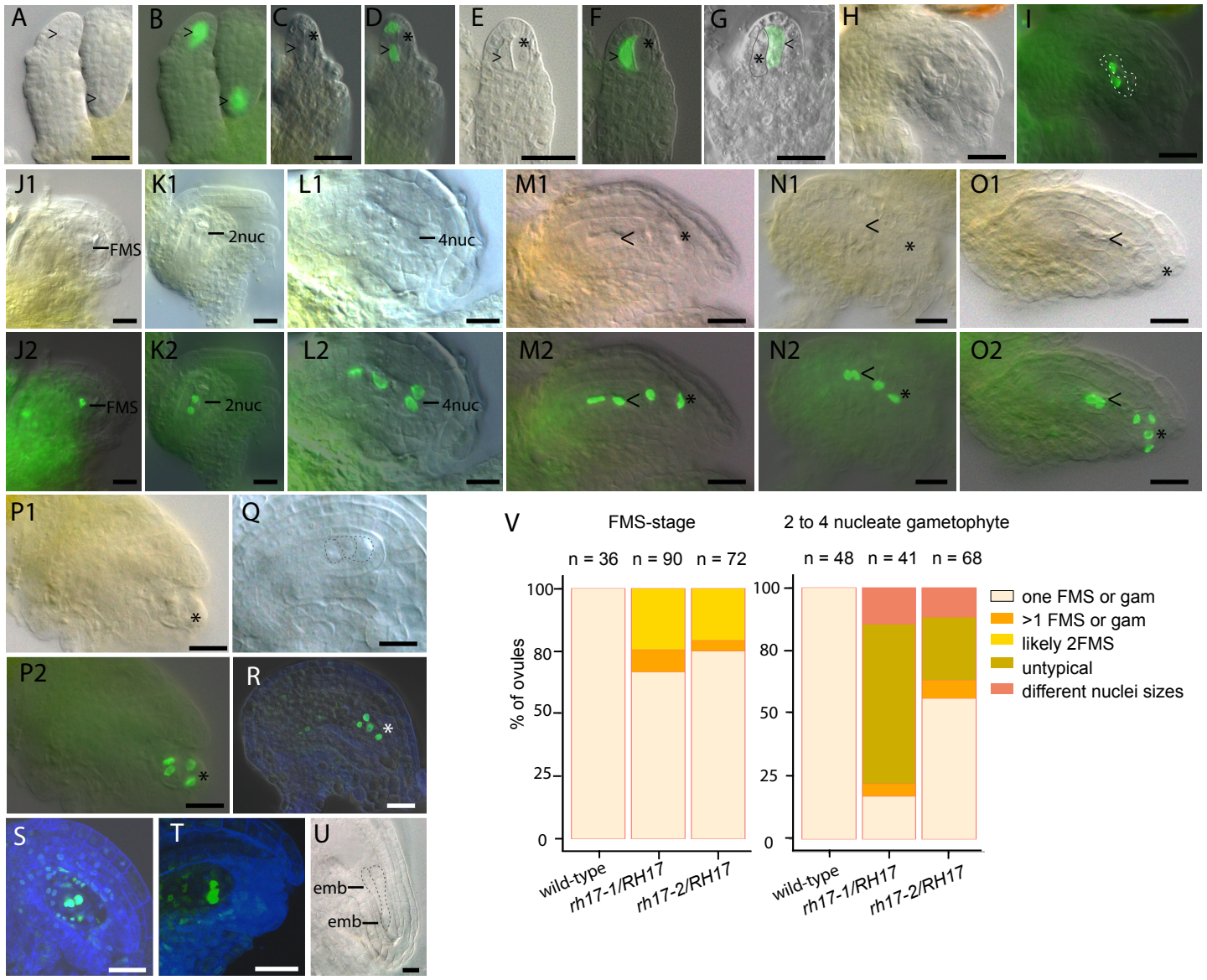

Fig. S3. Formation of more than one germline lineage per ovule. Epifluorescence microscopy (B, D, F, I, J2-O2, P2), (corresponding) DIC images (A, C, E, H, J1-O1, P1, Q, U), and laser scanning microscopy (G, R-T; blue signal: Renaissance 2200 cell-wall dye). MMCs are indicated by arrows, additionally enlarged cells are marked with a star. (A, B) Single MMCs in ovules of the p*KNU::nlsYFP* marker line serving as control. (C, D, G) Young ovules of *rh17-1/RH17*, and (E,F) *rh17-2/RH17*. (J-L) p*AKV::H2B-YFP* marker line used as control (Rotman et al., 2005). (M,O,R,S) Investigation of H2B-YFP activity driven by the *AKV*-promoter labelling gametophytic nuclei in *rh17-1/RH17*, and (N,P,T) *rh17-2/RH17*. Developing gametophytes are indicated by an arrow, ectopic gametophytes by a star. (S,T) Untypical positioning of nuclei likely indicates formation of two gametophytic lineages (counted as likely 2 FMS in V). (Q) Morphological investigation showing more than one FMS per ovule, and (U) two embryos in one seed in *rh17-2/RH17*. Scale bars are 20 µm. (V) Bar plot showing the frequencies of formation of additional gametophytic lineages, untypical numbers or positioning of gametophytic nuclei (untypical), or differences in sized of gametophytic nuclei observed based on H2B-YFP activity. Only ovules were scored in the category of more than one FMS or gametophyte when two cells were clearly distinguished. Differences in distributions of observations as compared to wild-type were confirmed for the lines carrying a mutant allele of *RH17* by fisher's exact test ($p < 0.001$). Per genotype, data from at least 4 plants are summarized.

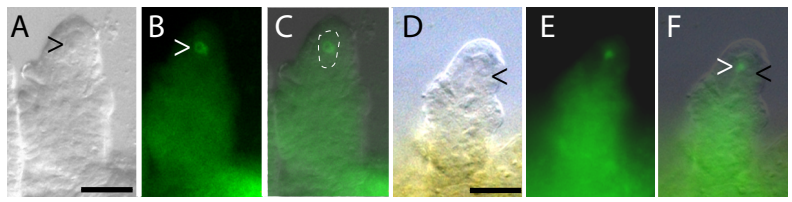

Fig. S4. REC8-mEGFP indicates meiosis of a single MMC in *rh17-1/RH17.* (A,D) DIC image of a MMC marked with an arrow. (B,E) Activity of *PRO*$_{REC8}$*:REC8:mGFP* (Prusicki et al., 2019) in a single MMC shown by epifluorescence microscopy, and (C,F) overlay with DIC image. Scale bars are 20 µm.

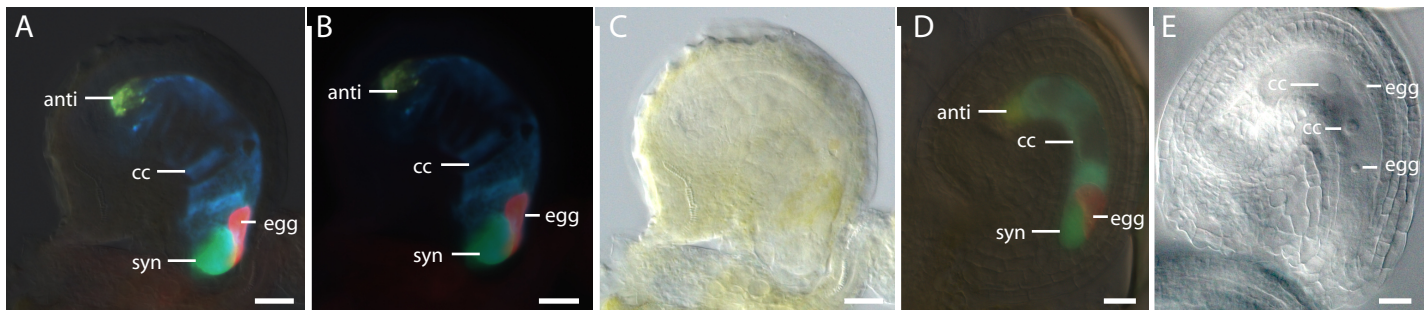

Fig. S5. Cell-type identities in mature gametophytes. Epifluorescence microscopy of representative ovules at 2-3 DAE (n = 95 and n = 62 gametophytes showing marker activity in *rh17-1/RH17* (A-C) and wild-type (D), respectively) expressing a quadruple-cassette labelling each cell of the mature gametophytewith a different fluorescent protein (Lawit et al., 2013): egg cell (egg) with DsRed, central cell (cc) with AmCyan, synergids (syn) with AcGFP, and antipodals (anti) with ZsYellow. (A,D) Overlay of DIC and fluorescent channels. (C) DIC image. (D) Clearing of mature ovule harboring two gametophytes in *rh17-2/RH17*. Scale bars are 20 µm.

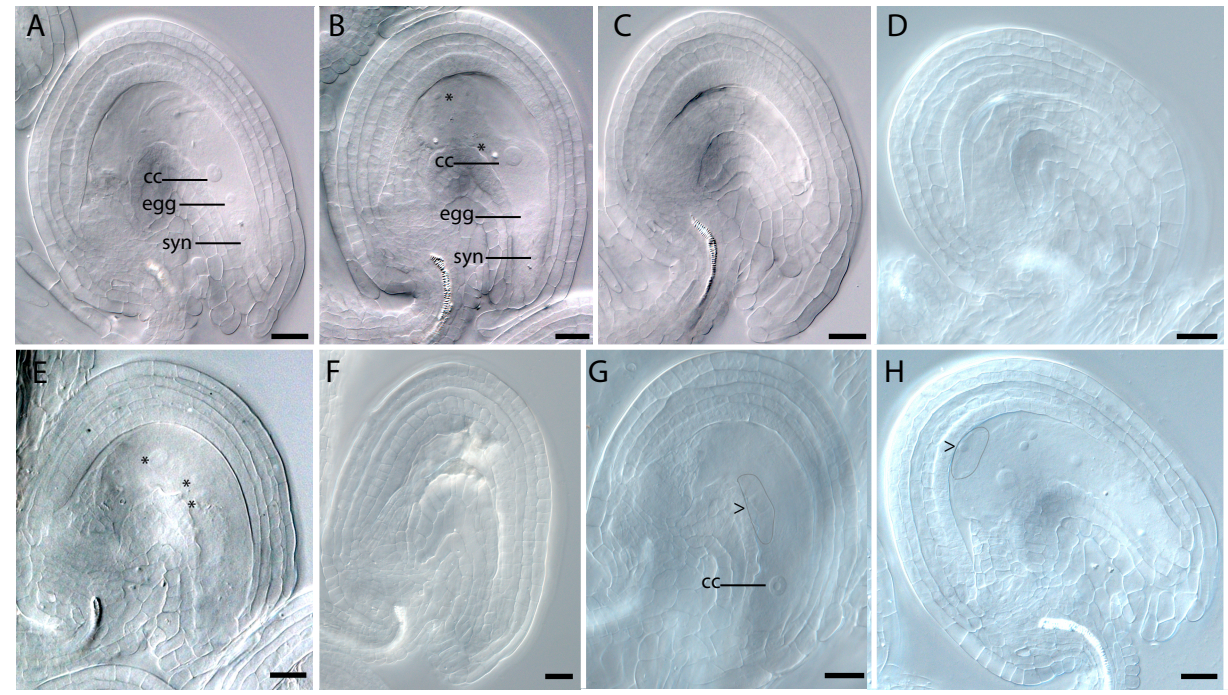

Fig. S6. Clearing of ovules at 5 DAE. (A-C) Wild-type, and (D-H) *rh17-1/RH17*. (A) Mature gametophyte. (B) Mature gametophyte with nuclei at chalazal end counted as “additional nuclei” which might represent antipodals (indicated by *). (C,D) Early developmental arrest of gametogenesis. (E) Features of autonomous endosperm (nuclei indicated by *). (F) Enlarged ovule showing features of parthenocarpy. (G,H) Ovules with additional gametophytes which have not reached maturity (indicated by >). egg egg cell, cc central cell, syn synergids; scale bars are 20 µm. (I) Box and whiskers plot summarizing observations for wild-type, *rh17-1/RH17*, and *rh17-2/RH17*.

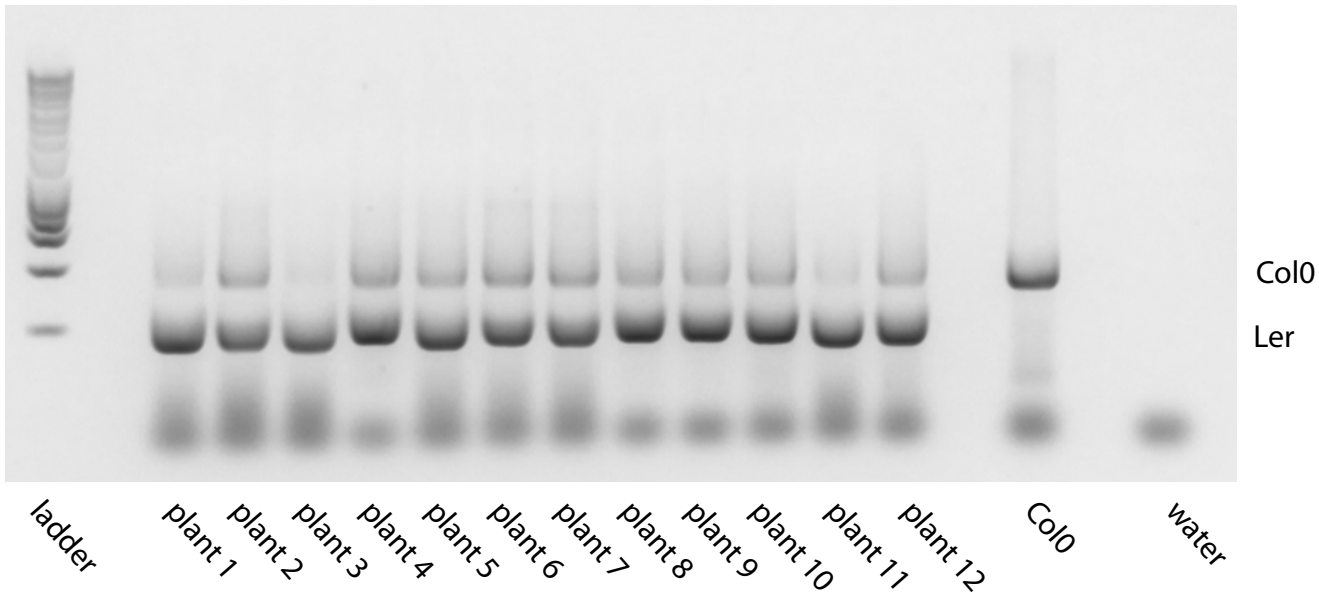

Fig. S7. Mapping approach shows hybrid identity in F1 offspring of *rh17-1/RH17* (Col-0) x L*er.*
Image of a 1% agarose gel stained with gelred showing amplification of Col-0 and Ler DNA genomic DNA from samples of 12 representative seedlings. Mapping primers T2E12F and T2E12R were used as described (Zhang et al., 2007), generating distinguishable band sizes for amplification products of each ecotype. As ladder Hyperladder I (Bioline) was used.

A

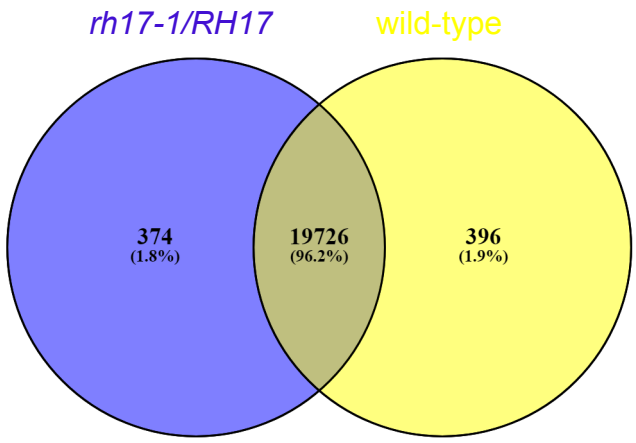

B

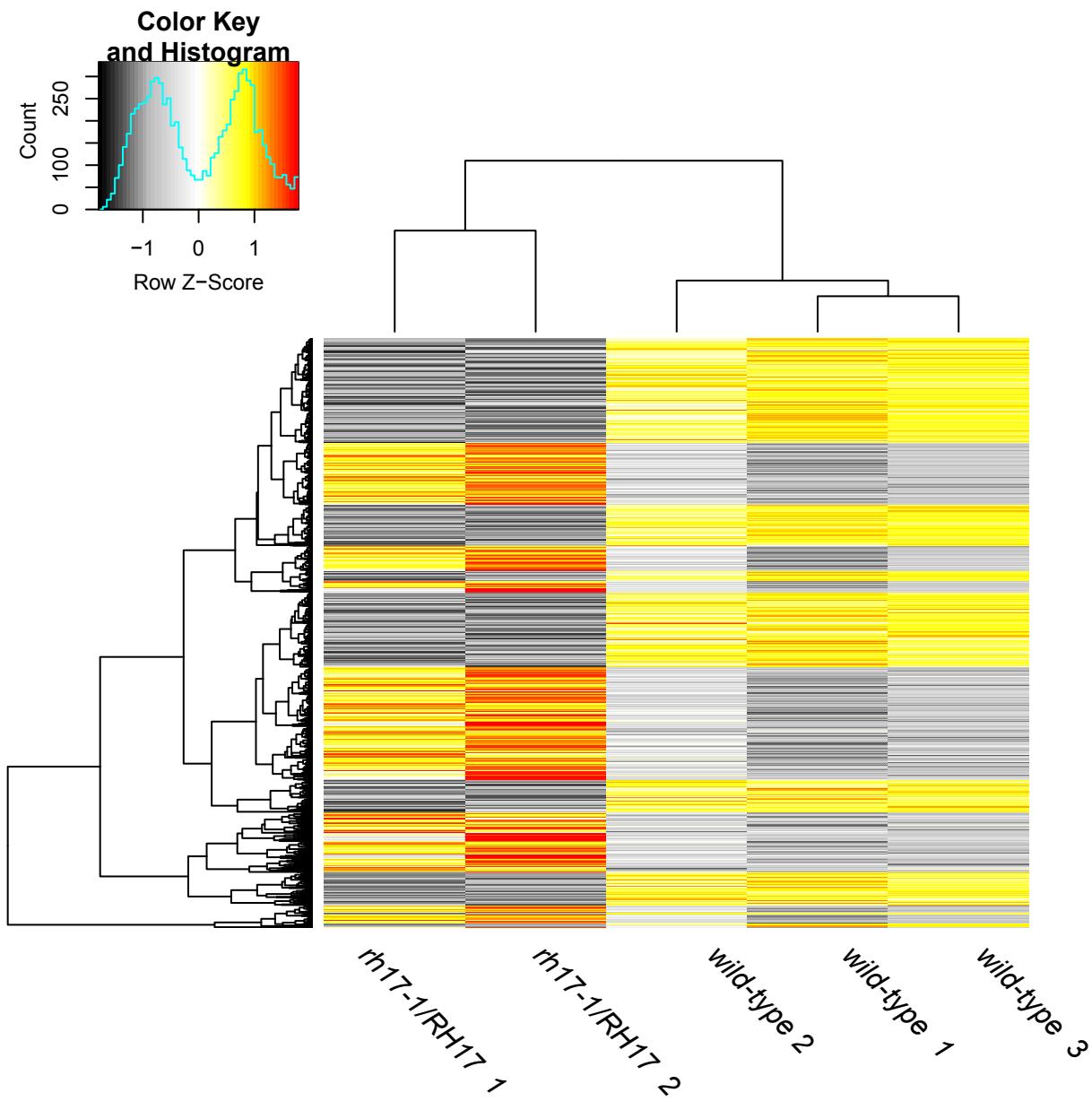

Fig. S8. Differential gene expression in ovules of *rh17-1/RH17* as compared to the wild-type at three days after emasculation. (A) Venn Diagram showing the overlap of genes expressed (> or = 10 read counts) in both samples of *rh17-1/RH17* or all samples of wild-type. (B) Heatmap based on log2-transformed TMM normalized read counts of 1'558 genes differentially expressed in samples from *rh17-1/RH17* as compared to wild-type as analyzed by EdgeR (Robinson et al., 2009). Hierarchical clustering of samples and genes was based on euclidean distance and hierarchical agglomerative clustering. Colors are scaled per row with red indicating high and black low expression.

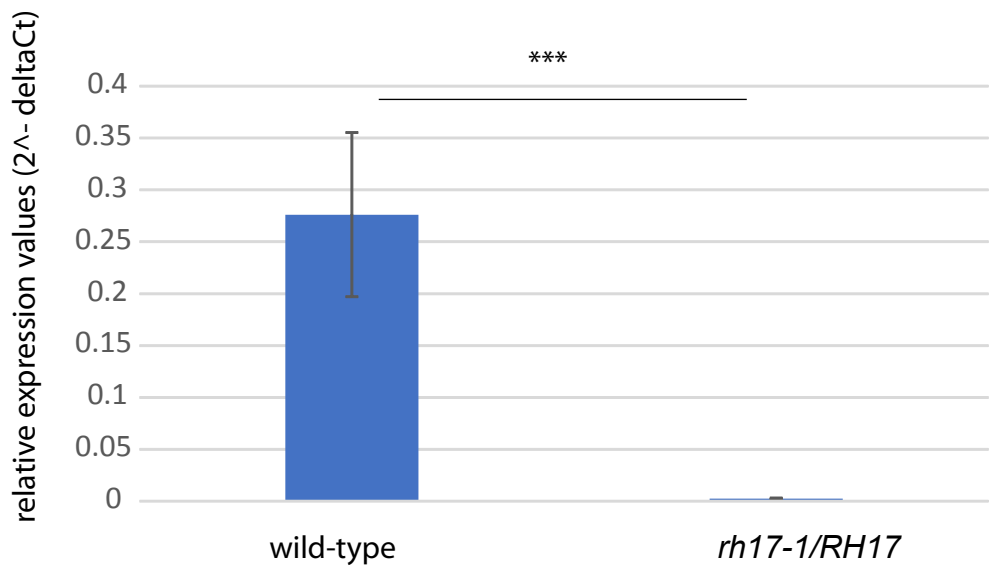

Fig. S9. Real time quantitative PCR. Relative expression levels of the long non-coding RNA AT1G07887 in ovules of wild-type as compared to *rh17-1/RH17* three days after emasculation. Shown are values averaged from three biological r eplicates and standard deviation. Significance of differences was inferred with students t-test ($p<0.001$).

Table S1. Summary of samples and mapping statistics. Given are for RNA-Seq libraries numbers of total raw reads and reads mapped to the A. thaliana reference genome, in addition to the numbers of genes mapped to exons using Star and counted with featureCounts (Dobin et al., 2013; Liao et al., 2014). Percentages refer to raw read numbers.

Click here to download Table S1

Table S2. TMM normalized read counts of 1’558 differentially expressed genes.

Click here to download Table S2

Table S3. Differential expression of genes in ovules of rh17-1/RH17 or wild-type at three days after emasculation.

Click here to download Table S3

Table S4. Gene ontology analysis to identify enriched biological processes.

Click here to download Table S4

Table S5. Genes represented in different enriched GO categories.

Click here to download Table S5

References

Dobin, A., Davis, C.A., Schlesinger, F., Drenkow, J., Zaleski, C., Jha, S., Batut, P., Chaisson, M., Gingeras, T.R. 2013. STAR: ultrafast universal RNA-seq aligner. *Bioinformatics (Oxford, England)* **29**, 15-21. **Kotliński, M., Knizewski, L., Muszewska, A., Rutowicz, K., Lirski, M., Schmidt, A., Baroux, C., Ginalski, K., Jerzmanowski, A.** 2017. Phylogeny-Based Systematization of Arabidopsis Proteins with Histone H1 Globular Domain. *Plant Physiol.* **174**, 27-34.
Lawit, S.J., Chamberlin, M.A., Agee, A., Caswell, E.S., Albertsen, M.C. 2013. Transgenic manipulation of plant embryo sacs tracked through cell-type-specific fluorescent markers: cell labeling, cell ablation, and adventitious embryos. *Plant Reprod*. **26**, 125-137.
Liao, Y., Smyth, G.K., Shi, W. 2014. featureCounts: an efficient general purpose program for assigning sequence reads to genomic features. *Bioinformatics* **30**, 923-930.
Liu, Y., Imai, R. 2018. Function of Plant DExD/H-Box RNA Helicases Associated with Ribosomal RNA *Biogenesis*. 9.
Lucas, M., Kenobi, K., von Wangenheim, D., Voβ, U., Swarup, K., De Smet, I., Van Damme, D., Lawrence, T., Péret, B., Moscardi, E., Barbeau, D., Godin, C., Salt, D., Guyomarc'h, S., Stelzer, E.H.K., Maizel, A., Laplaze, L., Bennett, M.J. 2013. Lateral root morphogenesis is dependent on the mechanical properties of the overlaying tissues. *Proc. Natl. Acad. Sci. U. S. A*. **110**, 5229-5234.
Prusicki, M.A., Keizer, E.M., van Rosmalen, R.P., Komaki, S., Seifert, F., Müller, K., Wijnker, E., Fleck, C., Schnittger, A. 2019. Live cell imaging of meiosis in Arabidopsis thaliana. *eLife* **8**, e42834.
Robinson, M.D., McCarthy, D.J., Smyth, G.K. 2009. edgeR: a Bioconductor package for differential expression analysis of digital gene expression data. *Bioinformatics* **26**, 139-140.
Ross, P., Slovin, J., Chen, C. 2010. A simplifed method for differential staining of aborted and non-aborted pollen grains. *Int. J. Plant Biol*. **1**, 2.
Rotman, N., Durbarry, A., Wardle, A., Yang, W.C., Chaboud, A., Faure, J.E., Berger, F., Twell, D. 2005. A novel class of MYB factors controls sperm-cell formation in plants. *Curr. Biol.* **15**, 244-248.
Schmidt, A., Schmid, M.W., Klostermeier, U.C., Qi, W., Guthorl, D., Sailer, C., Waller, M., Rosenstiel, P., Grossniklaus, U. 2014. Apomictic and sexual germline development differ with respect to cell cycle, transcriptional, hormonal and epigenetic regulation. *PLoS Genet.* **10**, e1004476.
Schmidt, A., Wuest, S.E., Vijverberg, K., Baroux, C., Kleen, D., Grossniklaus, U. 2011. Transcriptome analysis of the Arabidopsis megaspore mother cell uncovers the importance of RNA helicases for plant germline development. *PLoS Biol.* **9,** e1001155.
Zhang, Y., Glazebrook, J., Li, X. 2007. Identification of Components in Disease-Resistance Signaling in Arabidopsis by Map-Based Cloning. *Methods Mol. Biol.* **354**, 69-78.